Monitoring offshore wind farm power performance with SCADA data and advanced wake model

Niko Mittelmeier[1], Tomas Blodau[1], Martin Kühn[2]

[1]Senvion GmbH, Überseering 10, 22297 Hamburg, Germany

5 [2]ForWind – Carl von Ossietzky University of Oldenburg, Ammerländer Heerstraße 136, 26129 Oldenburg Germany

Correspondence to: Niko Mittelmeier (niko.mittelmeier@senvion.com)

Abstract. Wind farm underperformance can lead to significant losses in revenues. Efficient detection of wind turbines operating below their expected power output and immediate corrections help maximise asset value. The method, presented in this paper, estimates the environmental conditions from turbine states and uses pre-calculated look-up tables (LUTs) from

10 a numeric wake model to predict the expected power output. Deviations between the expected and the measured power output ratio between two turbines are an indication of underperformance. The confidence of detected underperformance is estimated by detailed analysis of uncertainties of the method. Power normalisation with reference turbines and averaging several measurement devices can reduce uncertainties for estimating the expected power. A demonstration of the method's ability to detect underperformance in the form of degradation and curtailment is given. Underperformance of 8% could be

15 detected in a triple wake condition.

1. Introduction

To increase confidence in offshore wind energy investments, investors need reliable wind turbines. The two pillars of system reliability are operational availability and the ability to achieve predicted power performance. In wind industry, the common standard IEC TS 61400-26-1 (2011) defines different categories of turbine conditions and describes the calculation of

20 availability. However within this standard the "Full Performance" category requires only the status of not being restricted in power production but there is no verification of the quality of the power performance.

The key to an economic investment is a function of quantity and quality. Quantity is linked to availability and wind turbines can provide lots of SCADA (supervisory control and data acquisition) information which enables analysis of time based

25 (IEC TS 61400-26-1, 2011) and production based availability (IEC TS 61400-26-2, 2014).

The quality of the power performance of a single turbine in specific conditions using a hub height met mast can be tested in accordance with the international standard IEC 61400-12-1 (2005). For most turbines in a typical wind farm, verification of the performance by comparison with the power curve is not suitable due to wake effects. And the installation and maintenance of a met mast is very expensive particularly offshore. Quantifying changes in power production based on wind

speed measurements from nacelle anemometry relies on the quality of the device itself and its transfer function which should account for the flow distortion behind the rotor. Using this approach still requires a wake free sector and leads to an increase in uncertainties. (Albers et al., 1999), (IEC 61400-12-2, 2013).

5   Efficient detection of underperformance of wind turbines increases asset value (Albers, 2004a). Incorrect turbine parameter settings, degradation of the blades, pitch or yaw errors all lead to less production than expected. We differentiate between degradation and curtailments. A curtailed turbine has a limited power output below its expected power. Possible reasons for curtailments are load or sound reductions or grid requirements. For these incidents, turbine parameters are changed on purpose and therefore documented in the turbines SCADA logs. A turbine that is degraded reaches rated power, but does not

10   fulfil its expected power curve. These kind of underperformance are more difficult to detect, especially when operating in the wake of neighbouring wind turbines.

Albers (2004b) has published two methodologies for wind turbine performance evaluation. His integral model uses available wind conditions from the energy production of neighbouring WTs, met masts or a combination of both and transfers the

15   information via flow modelling and wake modelling to the investigated wind farm. The measured yield is corrected for turbine availability and then compared against the modelled yield in absolute values. Due to high uncertainties this method is only proposed as a first general check. To reveal smaller deviations he proposes a relative wind turbine performance evaluation model. For this method, active power of direct neighbours are plotted against each other and by comparing two periods, changes can be evaluated. This method explicitly excludes the sectors where wakes are effecting one or both

20   turbines.

An international working group (IEC TC88 WG6, 2005) was trying to come up with a standard for wind farm power performance testing. The proposed method uses one or more met masts to establish a measured wind farm power curve matrix. This two dimensional measured power matrix (Wind direction, Wind speed) is compared against a modelled power

25   matrix taking wake effects into account (Mellinghoff, 2007)(Carvalho and Guedes, 2009). The standard could not be established.

Mittelmeier et al. (2013) presented a new method where not the absolute values between model and measurement are compared, but the relations between an observed turbine and all other turbines in the farm. In this way, the uncertainty of the

30   measurement chain could be reduced. The model is also based on pre-calculated power matrices which we call from now on "lookup-tables" (LUTs). Different wake models or even combinations of wake model results can be used to provide results for these LUTs. But the model relies on measurements from a met mast which is often not available. Furthermore, with increasing size of wind farms, the assumptions of one measurement position being representative for the whole offshore

wind farm is not valid (Dörenkämper, 2015). Further investigations are necessary to obtain a reliable and automated method to detect underperformance at individual turbines in a wind farm.

The purpose of this paper is to present the results of extending the wind farm performance monitoring method of Mittelmeier et al. (2013) by using SCADA instead of met mast data. A new combination of methods to obtain representative environmental conditions and further optimisation potential for wake models fine-tuned by SCADA data is presented and an estimation of the uncertainty of these methods is given.

In Section 2 the general approach of the method by Mittelmeier at al.(2013) is recalled. A new approach to generate a virtual met mast from SCADA data is explained in detail in Section 2.1. The wake model optimisations are described in Section 2.2. A closer look at the uncertainties of the method especially in relation to the establishment of a virtual met mast is discussed in Section 2.3. In Sections 3, 4 and 5 results for a demonstration case are presented, followed by a detailed discussion and the final conclusions.

2. Methods

To detect underperformance of a wind turbine, we estimate the expected turbine power ratio π (predicted power ratio) between the observed turbine and a reference turbine with a wake model for the actual condition and compare its result with the actual measured power ratio μ. A deviation between π and μ higher than a certain threshold indicates underperformance.

The performance monitoring model (Fig. 1) is based on two dimensional LUTs. The user can choose any wake model or even a combination of different model results to provide power output $P_{\pi i,j}$ values for different wind speed bin i and wind direction bin j. The predicted power output P_π is derived from the LUTs with linear interpolation knowing the measured wind speed and wind direction.

Information about the turbulence intensity, pressure, temperature and humidity from additional devices could be used to increase the dimensions of the power matrix and may add accuracy. As we are focusing on a monitoring method that uses only SCADA data, we will discuss and demonstrate one way to extract an useful wind speed and wind direction for this monitoring method in Section 2.1.

Commonly used power measurements are averages over 10-min periods. Due to the fact that there is a high scatter on power measurements for the same wind speed and wind direction bin, averaging a number N of 10-min samples is necessary until the power value converges to a satisfactory degree. The power matrix and N are derived in a pre-process as shown in Figure 1, which gives an overview on the whole performance monitoring process.

The power of the wind turbine under observation P_{ob} is divided by the power of a reference wind turbine P_{ref}. This leads to a normalized power curve with much lower slope in a wide range of partial load (See Figure 2) and therefore decreases sensitivity on wind speed measurement uncertainty. We define

$$\mu = \frac{1}{N}\sum_{n=1}^{N}\frac{P_{\mu ob_n}}{P_{\mu ref_n}} \text{ and} \tag{1}$$

$$\pi = \frac{1}{N}\sum_{n=1}^{N}\frac{P_{\pi ob_n}}{P_{\pi ref_n}}, \tag{2}$$

10 where $P_{\mu ob}$ and $P_{\pi ob}$ are the measured and predicted power of the observed turbine. $P_{\mu ref}$ and $P_{\pi ref}$ are the measured and predicted power of the reference turbine.

The underperformance indicator is defined as

$$\eta_{ob,ref} = 100\,\%\left(1 - \frac{\pi}{\mu}\right). \tag{3}$$

Having the measured power correlation in the nominator increases the sensitivity. The underperformance interval range of the indicator is in this way between $[0, -\infty[$. Non-operating turbine values have to be filtered out.

If $\eta_{ob,ref}$ is larger than the uncertainty (Section 2.3), underperformance has been detected. This correlation is repeated for
20 each combination of turbines which leads to $n\,(n-1)$ results (n = number of turbines in the farm). This adds further confidence to the detection, because an underperforming turbine will meet the criteria several times.

2.1 Determination of environmental conditions

2.1.1 Wind direction

The first step is to derive a wind direction ϑ for each 10-min interval. For our monitoring model we are using the absolute
25 wind direction signal from each turbine which is defined as

$$\vartheta = nacelle\ position + wind\ vane\ position\ . \tag{4}$$

The nacelle position is the angle between the rotor axis and a marking for true north. This marking is calibrated as part of the
30 commissioning. But often this signal is not maintained well during operation, because it has no effect on turbine

performance. This causes the necessity to apply an offset correction to this signal before using it for reanalysis purposes. The wind vane position indicates the angle of the flow to the rotor axis. It directly provides a value for the yaw error. The turbine controller uses this signal to control the yaw activity.

Within the Pre-Process (Fig.1) of the monitoring model we estimate the north marking offset for one turbine by checking the location of the maximum wake deficit with respect to the true north. Then we compare the average wind direction between corrected turbines and neighbouring turbines to estimate the remaining offset for all turbines. After applying this offset correction, the wind direction from all wind vanes are averaged in the complex plane to account for the wind direction discontinuity at the beginning/end of the value range, after removing outliers, outside ± 1.5 IQR (interquartile range).

2.1.2 Wind speed

Having determined an averaged wind direction we are now able to derive the averaged free flow wind speed. For this task we use the nacelle anemometry but only from wind turbines that are not affected by upwind turbines. To determine whether a turbine is affected by an upwind turbine or not we use the specification for power curve measurements from the international standard (IEC 61400-12-1, 2005). Each turbine location is checked against all other turbine locations according to the averaged wind direction. This is done within a Cartesian coordinate system were x represents the easting and y being the northing (See Figure 3). The wind turbine of interest WT_i is located at the position (x, y) and the turbine wake is from the turbine WT_0 at location (x_0, y_0).

$$\alpha = 1.3 \arctan\left(2.5\, \frac{D_n}{L_n} + 0.15\right) + 10 \tag{5}$$

is proposed by IEC 61400-12-1 (2005) and defines the width of the disturbed sector in degrees seen by the downwind turbine (the constants have the dimension of degree). D_n is the rotor diameter of the upwind turbine and L_n the distance between the two turbines defined by Eq. (5).

$$d_x = |x - x_0|,$$
$$d_y = |y - y_0|,$$
$$L_n = \sqrt{d_x^2 + d_y^2}, \tag{6}$$

With β, being the angle between the wake inducing turbine and the northing and the wind direction ϑ the turbine wake indicator γ can be described as:

$$\gamma = \begin{cases} |\beta + 360 - \vartheta| - \frac{\alpha}{2} & 0 < \beta < 90 \text{ and } 270 < \vartheta < 360 \\ |\beta - 360 - \vartheta| - \frac{\alpha}{2} & 270 < \beta < 360 \text{ and } 0 \leq \vartheta < 90 \\ |\beta - \vartheta| - \frac{\alpha}{2} & \text{else} \end{cases} \qquad (7)$$

The wind turbine of interest WT_i is categorized as waked turbine for $\gamma < 0$. The wind speed for the virtual met mast is therefore the average of the subset of the nacelle anemometer signals from all wind turbines with $\gamma > 0$.

2.2 The wake model

The wake model is a key factor in our performance monitoring method. Several benchmark tests have been published with a large variety of different models (Gaumond et al., 2012), (Réthoré et al., 2013) and (Steinfeld et al., 2015). And research is still ongoing to further improve prediction accuracy of such models.

In Figure 1 we highlight that the wake model and its tuning is part of the pre-process. The performance monitoring method itself is based on linear interpolation from the LUTs only. In (Mittelmeier et al., 2015), we have identified three key parameters for the tuning of the wake model (stability, wind direction uncertainty and wake drift). Figure 2 gives an example of how the different key parameters change the wake model results. The left plot visualises the active power of a turbine in wake normalised with a free flow condition in 6.3 D distance. The 0° on the *x*-axis locates the full wake situation according to the simulation. The right plot is a representation of the same data as normalised power curve with wind speed on the *x*-axis normalised with the wind speed, when wake effects fade away due to pitching activities of the upwind turbine.

In the first step, the wake model needs to be set up with the right atmospheric stability parameters. An increasing stability will cause higher wake losses and therefore shift the wake plot vertically down (from red rhombus to black triangles). The next two steps are applied on the wake model results which need to be calculated for a directional resolution of 0.5° and for each wind speed bin of 1 m/s. This resolution was proposed by Gaumond et al.(Gaumond et al., 2014) for his method to account for measurement uncertainties related to the wind direction which is the second key parameter in our tuning process. In his paper, three main sources of uncertainty are mentioned: The yaw misalignment of the reference turbine, the spatial variability of the wind direction within the wind farm and the variability of wind direction within the averaging of a 10 min interval. This causes a higher scatter in the data and leads to averaging effects that are not modelled in the simulation. In a post process each wind direction is averaged with weighted neighbouring results. A Gaussian distribution with a standard deviation σ_a has been proposed as a weighting function. The effect of this step is visualised in Figure 2 (red rhombus are without and orange points are with σ_a weighted averaging). In Mittelmeier et al. (2015), we could show, that for the prevailing conditions at Ormonde wind farm σ_a is a function of wind speed, decreasing with higher wind speeds.

Looking at the full wind rose for an AEP estimation, the Gaussian averaging has little impact on the result (Gaumond et al., 2014). But the smaller the wind direction bin size, the larger the prediction error made by the wake model. Hence it is crucial for our monitoring method to increase accuracy for smaller wind direction bin sizes which will decrease the uncertainty of the method.

5 The third tuning parameter is applying a simple offset on the wind direction of the LUTs to account for a drift of the wake. We call this phenomena from here on "wake drift". Fleming et al. (2013) has studied the effects of active wake control and in his baseline simulation (no yaw error) a small wake drift to the right can be observed when looking downwind. In the LES study of Vollmer et al. (2016) the wake drift increases from neutral to stable conditions also for 0° yaw angle. Gebraad (2014, p86) gives an explanation for the observations from the simulations by Fleming et al. (2013). The flow reacting on the

10 rotation of the rotor causes the wake to rotate counter clockwise (looking downstream). Higher wind speeds from the upper layer are transported downwards (on the left side) and lower wind speeds from the lower layer are pushed upward on the right side of the wake. As a result the velocity deficit at the right part of the wake increases, so the wake deflects to the right. Marathe et al. (2015) could show in their field measurement campaign with a dual-doppler radar the wake drifting to the right, as expected by the theory. But in the far wake they registered a movement to the left. The authors state the hypothesis

15 that this contradicting phenomenon may be caused by atmospheric streaks. In an offshore field experiment by Beck et al. (2015) further evidence is provided that wakes are moving out of the centre line. This wake drift is currently not modelled in Fuga and therefore applied in a further step of the pre-process (Fig. 1).

2.3 Uncertainties and underperformance criteria

It is essential to understand the uncertainties of the method to judge the confidence in underperformance detection. Any false

20 alarm can cause unnecessary trouble shooting.

For this evaluation, we follow the "Guide to the expression of Uncertainties in Measurements" (JCGM, 2008), which distinguishes between statistical Type A and instrumental Type B uncertainties. The important measurands of the method are the measured power and the predicted power for each wind turbine under observation and for reference $(P_{\mu ob}, P_{\mu ref}, P_{\pi ob}, P_{\pi ref})$. For the measured power P_μ we only use Type B, because each measurand is obtained from

25 different environmental conditions and therefore statistical Type A uncertainties are not applicable. The combined uncertainty can be derived with Eq. (8).

$$u_c(P) = \sum_{k=1}^{K}(c(P)_k u_k)^2 , \tag{8}$$

30 where c_k is the sensitivity factor and u_k the uncertainty of the k-th component of the measurement chain. For the predicted power P_π, we are using a combined uncertainty with statistical type A uncertainties, being the experimental standard deviation of the mean from the difference between wake model predictions and measurements and type B uncertainties

which conclude from the instrument devices to estimate wind speed and wind direction. Table 1 shows the uncertainty components of the predicted power P_π and provides the sensitivity factors, with $P_{\pi\,i,j}$ being the power value in the matrix referring to the wind speed bin i and the wind direction bin j. $V_{i,j}$ being the wind speed and $\vartheta_{i,j}$ being the wind direction of the element. In Table 2, the corresponding components for the uncertainty of the measured power P_μ are listed.

Results from the Offshore Wind Accelerator (Clerc et al., 2016) provide a range of 2.5% to 5% combined uncertainty for power curve verification based on a measurement chain that include a met mast and all its devices. The usage of LiDAR extends the range up to approximately 7%. In our case, the wake model will add further uncertainties which would lead to even higher values and therefore yields an inacceptable rate for underperformance detection. To lower this impact, the

10 monitoring method is based on normalised measurements and normalised predictions. An error at the estimated wind speed has a much lower impact on the ratio of the power of two turbines than on their absolute power performance. The uncertainty for Eq. (1) can be described as:

$$u(\mu) = u\left(\frac{P_{\mu ob}}{P_{\mu ref}}\right) =$$

$$= \frac{P_{\mu ref}}{P_{\mu ob}} \cdot \sqrt{\left(\frac{u_c(P_{\mu ob})}{P_{\mu ob}}\right)^2 + \left(\frac{u_c(P_{\mu ref})}{P_{\mu ref}}\right)^2} \;. \tag{9}$$

Equation (9) explains how to calculate the uncertainty of a summation in quadrature for division (Bell, 2001). The equation is equivalent for $u(\pi)$ and is applied on each 10-min sample.

With the two uncertainties $u(\mu)$ and $u(\pi)$ being independent the standard propagation of errors for η can be simplified
20 according to (Ku, 1966) to the following equation:

$$u^2(\eta) = \left(\frac{\partial \eta}{\partial \mu}\right)^2 u^2(\mu) + \left(\frac{\partial \eta}{\partial \pi}\right)^2 u^2(\pi) \;, \tag{10}$$

which leads to an uncertainty in η of:

$$u(\eta) = \frac{100}{\mu} \sqrt{u^2(\pi) + \left(\frac{\pi}{\mu}\right)^2 u^2(\mu)} \;. \tag{11}$$

The uncertainty derived by Eq. (11) can be displayed as a bandwidth around the underperformance indicator η, visualized in Fig. 4. Its magnitude is dependent on the sample size N. In Fig. 4 we obtain approximately 7 % uncertainty on the

performance ratio for $N > 1000$. The confidence level is one standard deviation, which is considered to be acceptable for underperformance detection.

In the next step we need to estimate the required number of power samples N for averaging (see Eq. (1) and Eq. (2)). This is directly linked with the earliest point in time when underperformance can be detected. We define this point as having a lower prediction error (with the optimal turbine operation model) than the prediction error derived by the model with the erroneous data taking the uncertainty into account.

3 Results and Demonstration

The objective of this paper was to present a developed method, using only SCADA data and pre-calculated numerical wake model results to detect underperformance at wind turbines in waked conditions within the wind farm. We have chosen the Ormonde wind farm to demonstrate the new method. The 30 turbines have a rated power of 5 MW and are owned by Vattenfall. The wind farm is located in the Irish Sea 10 km west of the Isle of Walney.

The farm layout displayed in Fig. 5 is structured in a regular array which allows comparison of several wake situations. The closest turbine spacing is in the range of 4.1 D to 4.3 D along the four rows orientated from north west to south east. We have selected a more frequent wind direction from south-south west where multiple columns of four turbines are aligned with a distance ranging from 6.3 D to 6.5 D. To simplify the demonstration of underperformance detection we focused on single wake, double wake and triple wake conditions behind turbine OR26 for a south-south westerly wind direction and a sector of 30° around the full wake situation. Two years of 10-min SCADA data were used to set up the performance monitoring model.

3.1 Environmental condition of demonstration wind farm

3.1.1 Wind direction

The wind direction is supposed to be representative for the wind turbines in the monitoring model. In our example, we have averaged up to 30 corrected wind direction signals for each 10-min interval. The variation among the individual signals provides an uncertainty estimate for this artificial wind direction. In Fig. 6, a histogram of the full data set of two years with each count being the difference between a single vane measurement and the corresponding mean wind direction for the averaged period is visualized. This variation can nicely be described by a Gaussian distribution with standard deviation of 3.6 °. This value is used for the uncertainty of the wind direction Table 1 is referring to.

3.1.2 Wind speed

Figure 7 demonstrates the quality of the virtual met mast derived with the methodologies described in Section 2.1.1 and Section 2.1.2. The average wind speed of all nacelle anemometers has been normalised by the averaged nacelle anemometer

wind speed of the wake free subset. The full data is binned into 2° and plotted against the averaged wind direction. The errors bars indicate the experimental standard deviation of the mean (JCGM, 2008). We obtain a quite good agreement with the Fuga model which has been used with a Gaussian averaging of standard deviation $\sigma_a = 4\,°$. So far there is no instruction available on how to determine this standard deviation which should take wind direction uncertainty into account (Gaumond

5   et al., 2014). We have chosen this value, because of a quite nice fit with the SCADA data. A linear regression between the wind speed of the standard model results (red dashed line) and the SCADA measurements equals $R^2 = 0.96$. The improved model (green solid line) gives an $R^2 = 0.97$.

When considering the demonstration sector of 30° around the full wake alignment behind wind turbine 26, the free flow

10   wind speed can also be described by a Gaussian distribution (Figure 8) with a standard deviation of 0.46 m/s.
This information is important for the investigation of the uncertainties Table 1 is referring to.

3.2 Wake model

For the demonstration of the described method, we used the Fuga wake model which uses linearized Reynolds Averaged Navier Stokes equations developed by Ott et al. (2011). With the second version of the software new features were added

15   (Ott and Nielsen, 2014) to account for different atmospheric stabilities and for wind direction uncertainties. The results for this paper have been produced with Fuga version 2.8.4.1. We have chosen this wake model for two reasons: Firstly, there is already a confident number of validations with measurements published (Gaumond et al., 2012), (Mortensen et al., 2013) and (Steinfeld et al., 2015) and secondly, the Gaussian averaging feature described by Gaumond et al. (Gaumond et al., 2014) is already implemented.

To get a more reliable monitoring model we need to calibrate the wake model settings and compare several different calculation results with measured SCADA data based on the established virtual met mast. The wake model is supposed to provide a two dimensional LUT (wind direction, wind speed) for each turbine. Further dimensions such as stability may improve the accuracy, but research and validation for these models are still ongoing. Therefore our calibrated model has to

25   be representative for the average annual conditions. Two full years of SCADA data have been used for this task.
We identified three steps to obtain a better match between the power modelled by the wake model Fuga and the measurements. Firstly, the standard deviation σ_a to account for the wind direction uncertainty was found to be decreasing with increasing wind speed. Secondly, the Fuga parameter to model the effect of atmospheric stability $\zeta_0 = 2.72E - 7$ was set to more stable conditions and thirdly, the centre of the wake was found to be drifting towards the right side when

30   traveling downwind. Approximately 2.5° in the single wake and an additional 1° is added with every turbine adding an additional wake to the flow. This results in a total offset of 4.5° for the triple wake referenced to the artificial wind direction from the virtual met mast (Section 2.1.1). One possible explanation for this behaviour is the fact, that the upwards moving blade diverts the flow with higher wind speeds downwards to regions with lower wind speeds and the downwards moving

blade causes the opposite. This results in a higher wind speed on the left side than on the right side of the wake and leads to a drift of the wake centre. A second explanation can be derived from the Coriolis force, which leads to an increased force to right (northern hemisphere) on accelerating air particles. We cannot fully rule out the possibility of an unwanted yaw misalignment as the uncertainties within this process of aligning the turbine lies within 3° (IEC 61400-12-2, 2013). But a single wake drift of 2.5° is also within the simulation results for 0° yaw misalignment at stable conditions (Vollmer et al., 2016).

Figure 5 shows the location and layout of the demonstration wind farm. The column of turbines behind turbine OR26 has been selected for the validation of the wake model settings. The benchmark are simulations for neutral conditions with none of the post processing's mentioned in section 2.2 to take wind direction uncertainty, atmospheric stability and wake drifts into account. Figure 9 demonstrates the improvement of model prediction and its capabilities for single wake, double wake and triple wake situation. The left column visualises wake deficit plots where the power has been normalized with the free flow turbine, as function of the wind direction, centred to the full wake. The data is filtered for wind speed of 8±1 m/s. The right column are normalized wake power curves. The power, normalized with free flow power, is shown as function of the wind speed, normalized with wind speed at rated power for the turbine in the wake. These data have been filtered for a wind direction sector of 5°. The optimised simulation results with the green diamonds follows the SCADA data with the black dots much closer than the benchmark case marked as red triangles. The error bars indicate one standard deviation of the measured SCADA data at each bin. The three fine-tuning steps decreased the power prediction error in a full wake with ±5° sector width from 7% to 1.5%(Mittelmeier et al., 2015) for the presented case.

Having now an optimised wake model, the first two steps of the pre-process (Figure 1) are accomplished and the matrices for the "predicted power" can be established. In the next Section, the detection of underperformance will be demonstrated with two test cases.

3.3 Demonstration Case

Two years of SCADA data have been contaminated with two different error types. The first manipulation simulates a degradation of 8 % of its power production for which the original data set that has been used to calibrate the model, is multiplied by 0.92. According to the findings in Section 2.3 a degradation of 8 % is just high enough to distinguish from the uncertainties of a turbine in triple wake. The second test case is a simple power curve curtailment at 60 % rated power.

In Figure 10 the normalized power as function of the normalized wind speed is shown in a scatterplot. The coloured points in green represent correct turbine performance (P_optimal). The yellow dots (P_degraded) describe the degradation and the red dots (P_curtailed) are the data with the curtailment. Measurements from above rated wind speed are removed to concentrate on the part of the power curve where underperformance is more difficult to detect.

Below 5m/s we have realized a strong increase in wind direction variation among the turbines compared to the artificial wind direction from the virtual met mast. This variation increases the uncertainty of the model and therefore it is filtered out.

To further increase the certainty of the result, we calculate the underperformance indicator for each turbine with any other possible combination of reference turbine. For the whole wind farm of 30 turbines this leads to 870 combinations. For simplification in this demonstration, we are only focussing on the four turbines in the row behind turbine OR26.

At first, we need to estimate the required number of power samples N for averaging. This is directly linked with the earliest point in time when underperformance can be detected. We define this point by having a lower prediction error with the optimal turbine operation model than the prediction error derived by the model with the erroneous data taking the uncertainty into account. This can be visualized in Figure 11. The graphs present the accumulated level of underperformance η as function of the number of samples (N values). The data with the error appears in a solid line and grey uncertainty margin. The dashed green line represents the data with the turbine in optimal operation. The lowest quantity N, where the "optimal" (green dashed) line confirms a lower η than the border of the grey area, is the point where we highlight underperformance with sufficient certainty. Figure 11 demonstrates the two test cases with a turbine under curtailment at different wake situations and the corresponding situation for a degraded turbine. A wake model bias has been corrected in such a way, that the results for the optimal turbine prediction with the full two years data equals to zero.

In Table 3 we have listed the N values which are necessary to measure for each case until underperformance can be detected with sufficient certainty. They can be translated into hours by $N/6$ as we are using 10-min averages.

Figure 12 is a graphical representation of the development of uncertainty with increasing number of averaging data. The free flow has a comparatively low uncertainty in comparison with the three wake situations. All four graphs have higher uncertainty in the beginning and quickly decrease with increasing N. At approximately $N = 150$ the uncertainty of all three wake states has dropped at least once below 8 %. With $150 < N < 500$, $u(\eta)$ is still very unstable and stretches between 8 % and 10 %.

A clear additional drop, even below 7 %, can be seen from $500 < N < 1000$. Beyond $N > 1000$, $u(\eta)$ stabilizes towards a more and more horizontal line. In Table 4 the corresponding uncertainty for the estimated first time of detection is listed.

The power curve scatter plot of all four wake conditions with the number of quantities, necessary for detection are visualized in Figure 13.

4. Discussion

The model was able to detect the selected demonstration error cases after a certain averaging time. With the proposed sources of uncertainty and the described method to obtain a combined level a very clear increase of uncertainty can be seen from free flow to wake condition cases. The reason for this behaviour can be led back to the normalization procedure. The largest source of uncertainty is usually the wind speed measurement, followed by the wind direction measurement (category B uncertainties). Looking at the sensitivity factor for both readings, which are based on the slope of the quotient between neighbouring normalized LUTs cells, they approximately equal to zero for the free flow case. Therefore only category A uncertainties are left, which quickly decrease with increasing number of measured values N.

In our example, the curtailment took less than 170 values to be detected (see Table 3). This of course is very dependent on the wind distribution. The wind has to be high enough to force the turbine into the underperformance. At rated wind, detection is much faster than at wind varying around the power limitation. The right column in Table 3 is showing the total values N and in brackets the values considering only wind speeds high enough to force the turbine into the curtailment. The N values in Table 3 increase with each additional wake added to the flow. Furthermore, the figures show that curtailments (values in brackets) can be detected earlier than degradation.

The tuning of the wake model is an essential part of the method. The key tuning parameters have been estimated by trying to obtain the best fit with the SCADA data. This is a clear weak point of the method and further investigations are necessary to find ways to predict the right settings without measured data. Without such tuning, each of these parameters will contribute as an additional source of uncertainty and therefore reduce the accuracy. A further improvement could be to extend the dimensions of the LUTs with atmospheric stability. Dörenkämper et al. (2012) could show that the influence on the development of wind turbine wakes is measurable. A link from SCADA data to atmospheric stability would be needed. An investigation is planned for future work.

The sensitivity of the underperformance indicator η states the measured power correlation in the nominator of Eq. (3). In this way the interval range increases from $[0, -100]$ to $[0, -\infty[$. Division with 0 is prevented by filtering non-operating conditions. The increased interval leads to a higher sensitivity and therefore further reduces the N values for the first underperformance detection.

Using wind speed and wind direction measurements derived from a large number of devices can lead to acceptable levels of uncertainties although each single device for itself has comparably high uncertainties as described in more detail in the power verification standard using nacelle anemometry (IEC 61400-12-2, 2013). The stated uncertainties for wind speed and wind direction may be sufficient for the relative comparison to detect underperformance between turbines but it does not

meet the requirements for an absolute performance validation according to IEC 61400-12-1 (2005) or IEC 61400-12-2 (2013). One could perform power curve verification test in accordance with the mentioned standards at turbines where they are applicable and those turbines being reference turbines in the monitoring method would increase the confidence in underperformance detection. At least for the concurrent period.

5. Conclusion

A method for offshore wind farm power performance monitoring with SCADA data and advanced wake models was introduced. Wind speed and wind direction have been extracted from all devices in the wind farm to obtain a global measurement for the whole wind farm. In this way, the level of uncertainty could be lowered compared to a single nacelle measurement. Furthermore the uncertainties in performance level prediction could be reduced by normalization and referencing correlations. A suitable wake model was chosen, calibrated with SCADA data and used in a demonstration case. A procedure to determine the optimal number N of 10-min samples to detect underperformance with sufficient certainty has been presented. Here the method was capable of detecting a degradation of 8 % in a triple wake situation with the confidence of one standard deviation. The described method can be used after a wake model recalibration with approximately two years of wind farm SCADA data. This can enable a real time monitoring from then on for the rest of the operational lifetime.

Acknowledgement

The presented work is partly funded by the Commission of the European Communities, Research Directorate-General within the scope of the project "ClusterDesign" (Project No. 283145 (FP7 Energy)).

We would like to thank Vattenfall Wind Power and Senvion SE for making this investigation possible.

Furthermore we would like to thank the R Core Team for developing the open source language R (R_Core_Team, 2015).

References

Albers, A.: Efficient wind farm performance analysis, in DEWEK, Deutsche WindGuard Consulting GmbH., 2004a.

Albers, A.: Relative and Integral Wind Turbine Power Performance Evaluation, in EWEC, London., 2004b.

Albers, A., Klug, H. and Westermann, D.: Power performance verification, in EWEC, Nice. [online] Available from: http://www.dewi.de/dewi/fileadmin/pdf/publications/Publikations/albers_powerperformance_ewec99.pdf, 1999.

Beck, H., Trujillo, J. J., Wolken-möhlmann, G., Gottschall, J., Schmidt, J., Peña, A., Gomes, V., Lange, B., Hasager, C. and Kühn, M.: Comparison of simulations of the far wake of alpha ventus against ship-based LiDAR measurements, in RAVE Conference., 2015.

Bell, S.: A Beginner's Guide to Uncertainty of Measurements, Meas. Good Pract. Guid., 11(2), 41, 2001.

Carvalho, H. and Guedes, R.: Wind Farm Power Performance Test , in the scope of the IEC 61400-12-3, in Wind Power Expo, Chicago., 2009.

Clerc, A., Stuart, P., Cameron, L., Feeney, S. and Fnc, I. C.: Results from the Offshore Wind Accelerator (OWA) Power Curve Validation using LiDAR Project, in Wind Europe Workshop "Analysis of operating wind farms.", 2016.

5 Dörenkämper, M.: An investigation of the atmospheric influence on spatial and temporal power fluctuations in offshore wind farms, PhD Thesis., University of Oldenburg., 2015.

Dörenkämper, M., Tambke, J., Steinfeld, G., Heinemann, D. and Kühn, M.: Influence of marine boundary layer characteristics on power curves of multi megawatt offshore wind turbines, in DEWEK, pp. 1–4, DEWEK., 2012.

Fleming, P. A., Gebraad, P. M. O., Lee, S., van Wingerden, J. W., Johnson, K., Churchfield, M., Michalakes, J., Spalart, P. 10 and Moriarty, P.: Evaluating techniques for redirecting turbine wakes using SOWFA, in ICOWES2013 Conference., 2013.

Gaumond, M., Réthoré, P. and Bechmann, A.: Benchmarking of wind turbine wake models in large offshore wind farms, in the Science of Making Torque from Wind Conference, Oldenburg., 2012.

Gaumond, M., Réthoré, P., Ott, S., Pena, A., Bechmann, A. and Hansen, K. S.: Evaluation of the wind direction uncertainty and its impact on wake modeling at the Horns Rev offshore wind farm, Wind Energy, 17, 1169–1178, doi:10.1002/we.1625, 15 2014.

Gebraad, P. M. O.: Data-Driven Wind Plant Control, 2014.

IEC 61400-12-1: Power performance measurements of electricity producing wind turbines., 2005.

IEC 61400-12-2: Power performance of electricity-producing wind turbines based on nacelle anemometry., 2013.

IEC TC88 WG6: Wind farm power performance testing working group draft, IEC TC88 WG6 DRAFT, IEC., 2005.

20 IEC TS 61400-26-1: Time-based availability for wind turbine generating systems., 2011.

IEC TS 61400-26-2: Wind turbines – Part 26-2: Production-based availability for wind turbines., 2014.

JCGM: Evaluation of measurement data — Guide to the expression of uncertainty in measurement, First Ed. Sept. 2008, 2008.

Ku, H.: Notes on the use of propagation of error formulas, J. Res. Natl. Bur. Stand. (1934)., 70C(4), 263–273, 1966.

25 Marathe, N., Swift, A., Hirth, B., Walker, R. and Schroeder, J.: Characterizing power performance and wake of a wind turbine under yaw and blade pitch, , doi:10.1002/we, 2015.

Mellinghoff, H.: Wind Farm Power Performance Verification, DEWI., 2007.

Mittelmeier, N., Amelsberg, S., Blodau, T., Brand, A., Drueke, S., Kühn, M., Neumann, K. and Steinfeld, G.: Wind farm performance monitoring with advanced wake models, in Proceedings of the EuropeanWind Energy Association Offshore 30 Conference, Frankfurt., 2013.

Mittelmeier, N., Blodau, T. and Kühn, M.: Offshore wake model validation – Methodology for linking model results and operational data, in DEWEK., 2015.

Mortensen, N. G., Nielsen, M. and Jørgensen, H. E.: First Offshore Comparative Resource and Energy Yield Assessment Procedures (CREYAP)., 2013.

35 Ott, S. and Nielsen, M.: Developments of the offshore wind turbine wake model Fuga, Report E-0046, DTU Wind Energy., 2014.

Ott, S., Berg, J. and Nielsen, M.: Linearised CFD Models for Wakes, Risø National Laboratory, Roskilde, Denmark., 2011.

R_Core_Team: R: A Language and Environment for Statistical Computing, [online] Available from: https://www.r-project.org/, 2015.

Réthoré, P., Hansen, K. and Barthelmie, R.: Benchmarking of wind farm scale wake models in the EERA-DTOC project, Int. Conf. Aerodyn. Offshore Wind Energy Syst. wakes, (June), 2013.

5   Steinfeld, G., Mittelmeier, N., Drüke, S., Brand, A., Hait, T. and Amelsberg, S.: Report on the results of benchmarks for wake models. [online] Available from: www.cluster-design.eu, 2015.

Vollmer, L., Steinfeld, G., Heinemann, D. and Kühn, M.: Estimating the wake deflection downstream of a wind turbine in different atmospheric stabilities: An LES study, Wind Energy Sci. Discuss., (September), 1–23, doi:10.5194/wes-1-129-2016, 2016.
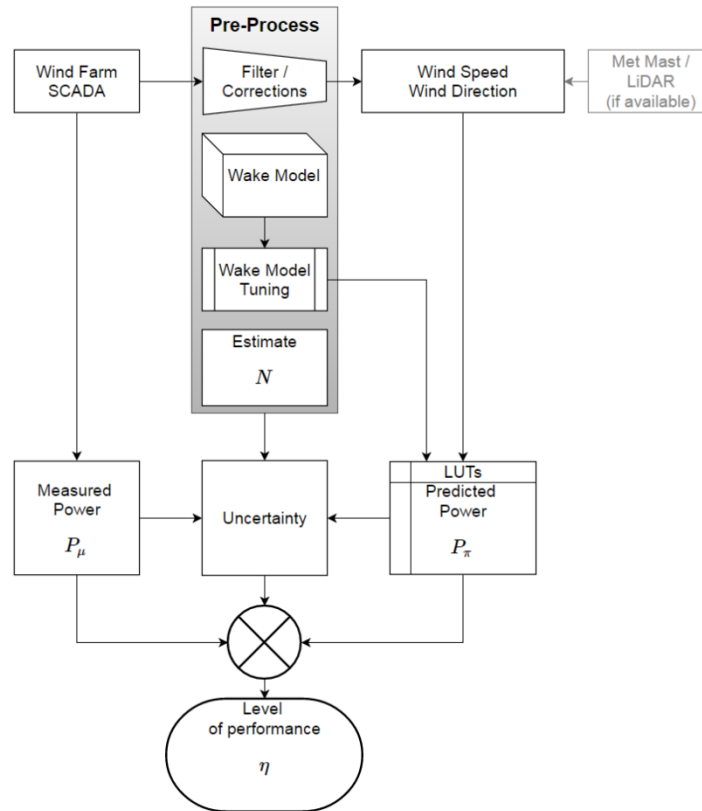
Figure 1: Flowchart of the Performance Monitoring Model. Wind speed and wind direction are derived from SCADA data after an offset correction of each wind direction signal and outlier filtering. Wake model calculations and tuning as well as the estimation of the number N of 10-min samples for averaging are pre-processed. N, P_π and P_μ are input values for the uncertainty
15   **calculation. An underperformance indicator η lower than the uncertainties indicates underperformance.**
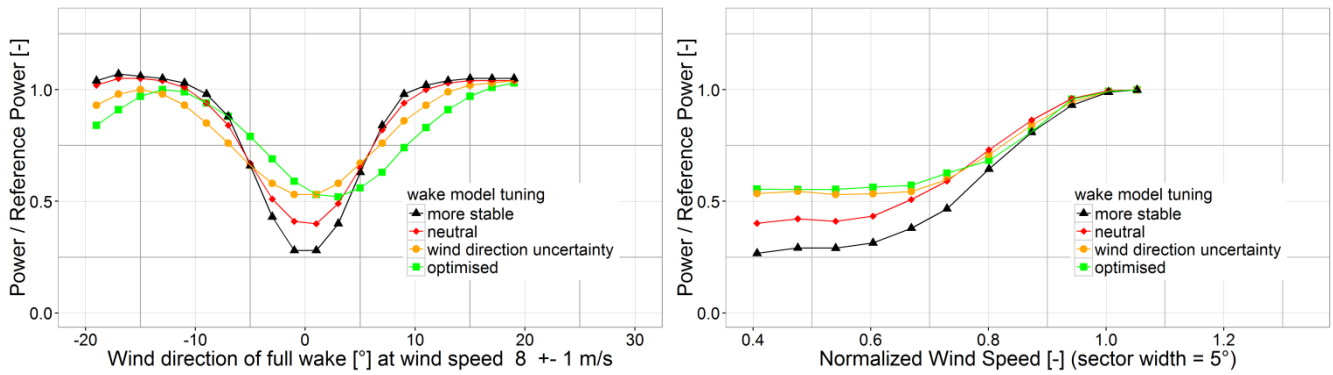
Figure 2: Impact of different key tuning aspects on the wake model results step by step. An increasing atmospheric stability increases the wake deficit (from red rhombus to black triangles). Wind direction uncertainty flattens the wake deficit (orange points), and a wind direction bias shifts the deficit horizontally (green squares). The left plot shows the power of the turbine in the wake divided by the power of a turbine in free flow conditions as function of the wind direction. The right plot displays the same power ratio as function of the normalized wind speed. (normalized power curve)
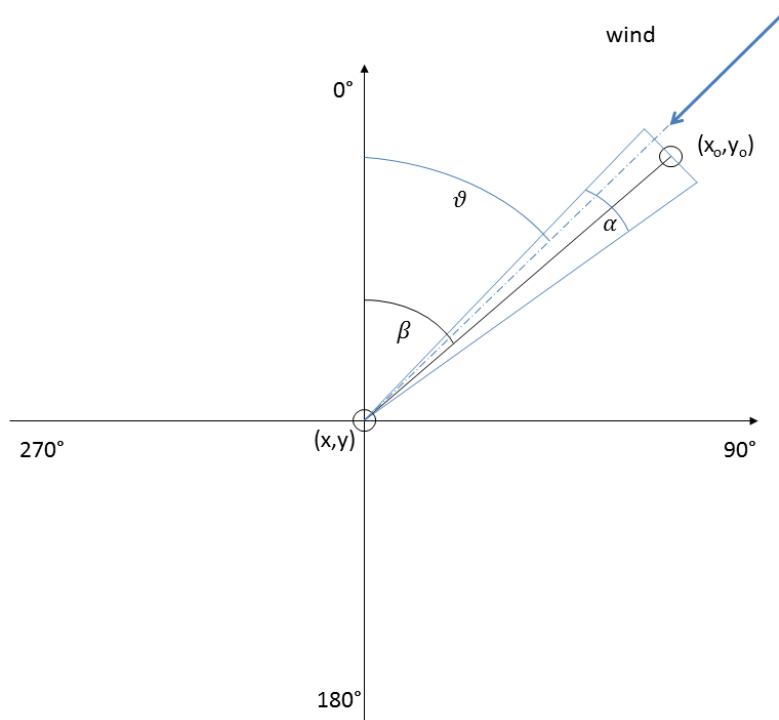
Figure 3: Determination of free flow turbines for wind speed averaging. The turbine at $(x0,y0)$ produces a wake on the turbine at (x,y) for the displayed wind direction ϑ. β is the angle between the orientation of the turbines and the true north. α is the angle of the disturbed sector in accordance with IEC 61400-12-1.
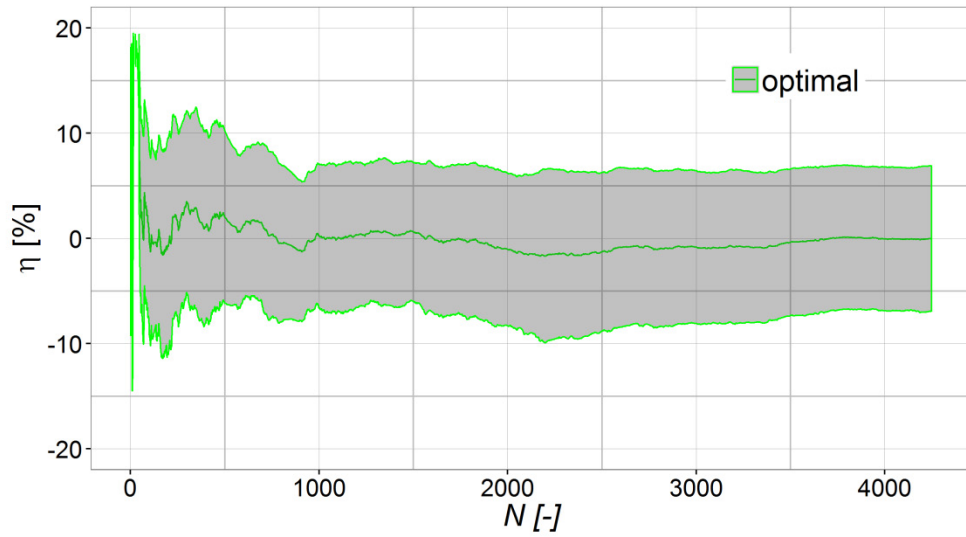
Figure 4: Underperformance indicator η with uncertainty margin as function of the number of measurement values *N*. Derived with the calibrated model at a turbine in triple wake.
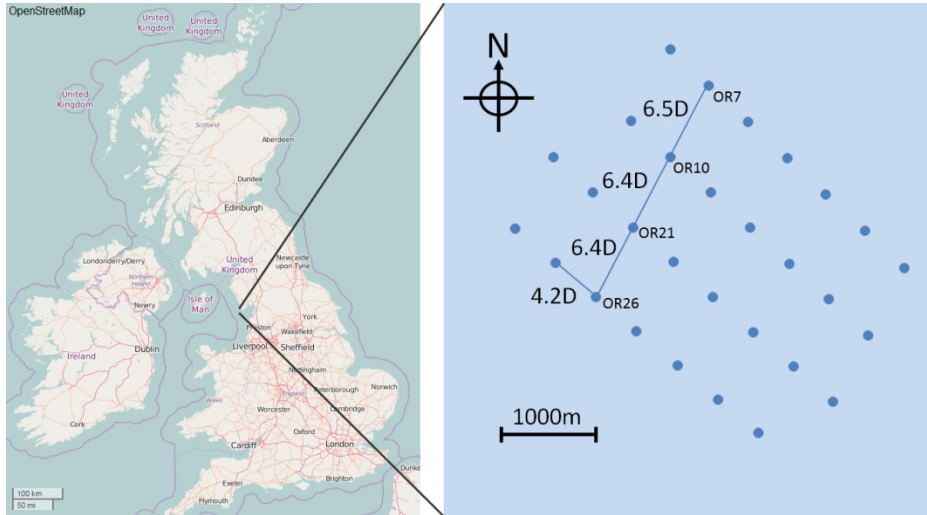
5   **Figure 5: Layout of wind farm Ormonde. The 30 turbines of 5 MW class are located in the Irish Sea 10km west of the Isle of Walney. For a wind direction of 207 ° the single wake, double wake and triple wake behind OR26 has been selected as underperformance demonstration cases.**
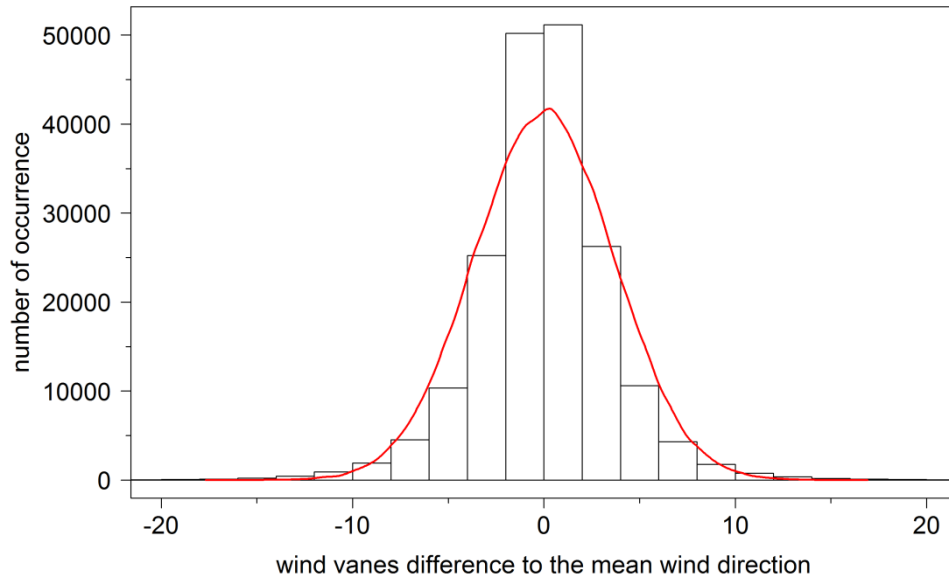
Figure 6: Estimation of uncertainty of the artificial wind direction. Histogram of the deviation of 30 individual wind vanes from the average wind direction for the full data set filtered for wind speeds > 5m/s with a sector of 30 ° centring the full wake condition. The red curve represents a Gaussian fit with a standard deviation of 3.6 °.
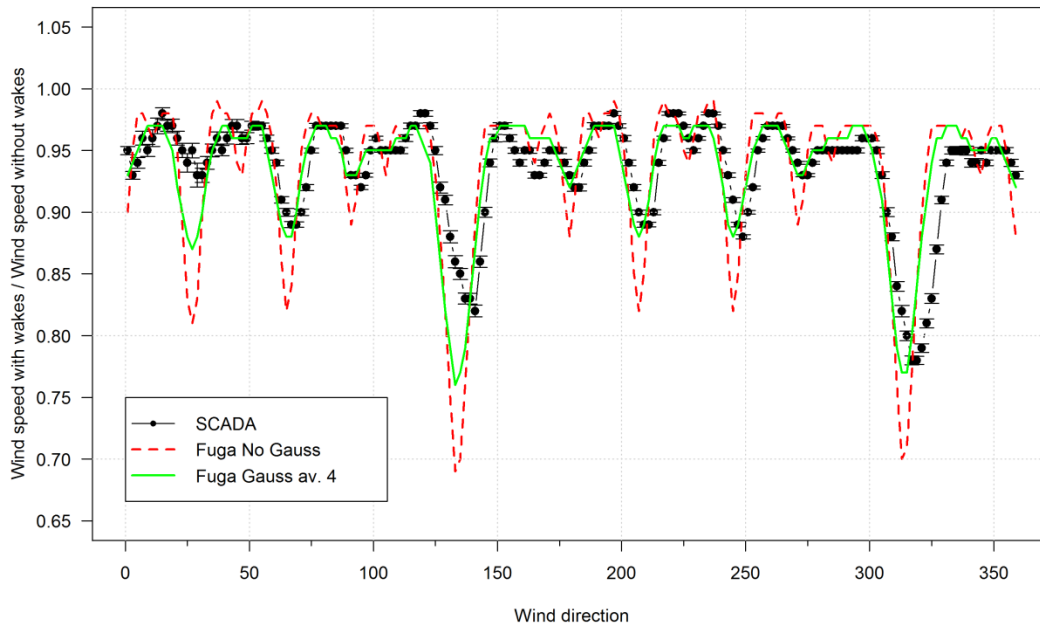
Figure 7: Wind farm averaged wind speed with wake effects normalised with wind farm averaged wind speed without wake effects plotted versus averaged wind farm wind direction. Black dots show the measurements from SCADA and the green solid line represents the results from Fuga with a Gauss averaging for standard deviation of 4°. An offset of the wind direction between model and SCADA can be observed. At 207 ° the offset is approximately 2.2 ° and it increases up to 5 ° for wind directions (132 ° and 312 °) with the largest wake effects. An explanation and correction for this "wake drift" is proposed in section 2.2.
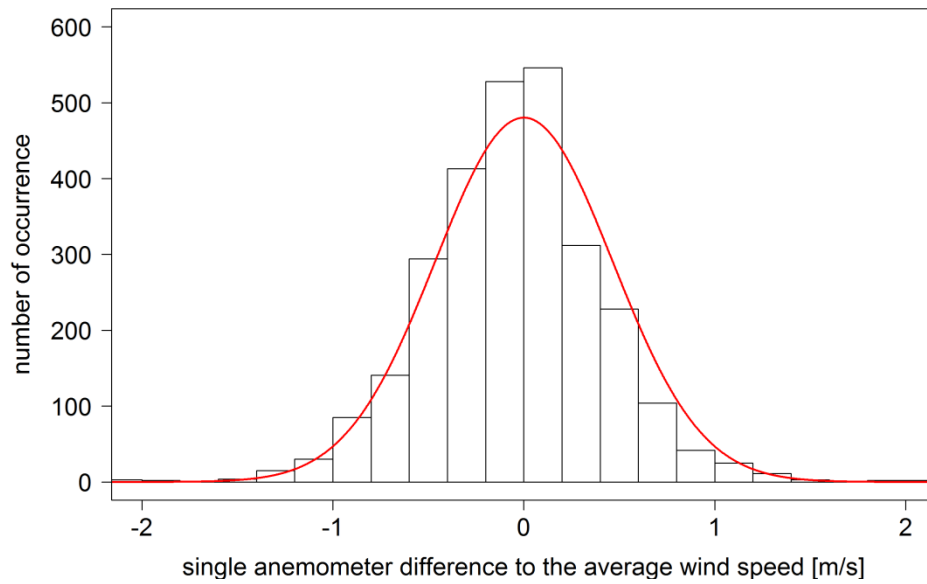
Figure 8: Estimation of uncertainty of the artificial wind speed. Histogram of the wind speed difference of a single anemometer to the average wind speed of all free flow anemometers. The displayed Gaussian distribution (red line) has the standard deviation of 0.46 m/s. A sector of 30 ° centring full wake alignment has been selected.
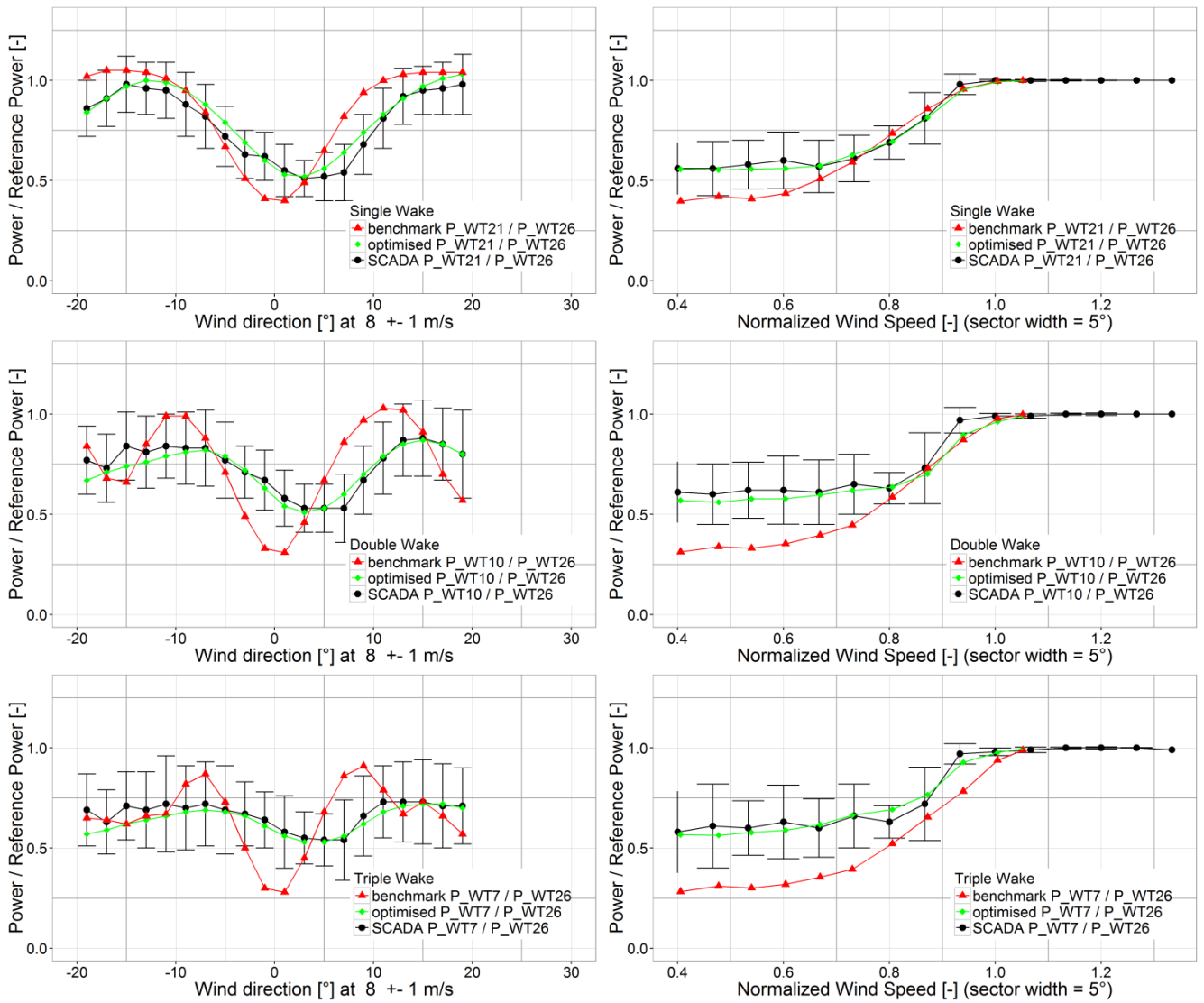
Figure 9: Tuning of the wake model results.(left column) Power normalized by the power of the free flow turbine as function of the wind direction centred at full wake for 8 ± 1 m/s wind speed. (right column) Power normalized by the power of the free flow turbine as function of the wind speed normalized by wind speed at rated power for the waked turbine. Black dots represent the measured and binned SCADA data with error bars of one standard deviation. The red triangles show wake model results with Fuga standard settings ($\zeta_0 = 0$, no Gaussian averaging) and the green diamonds provide the tuned results. ($\zeta_0 = 2.72E - 7$, Gaussian averaging as function of the wind speed and applying the wind direction offset to account for the wake drift).
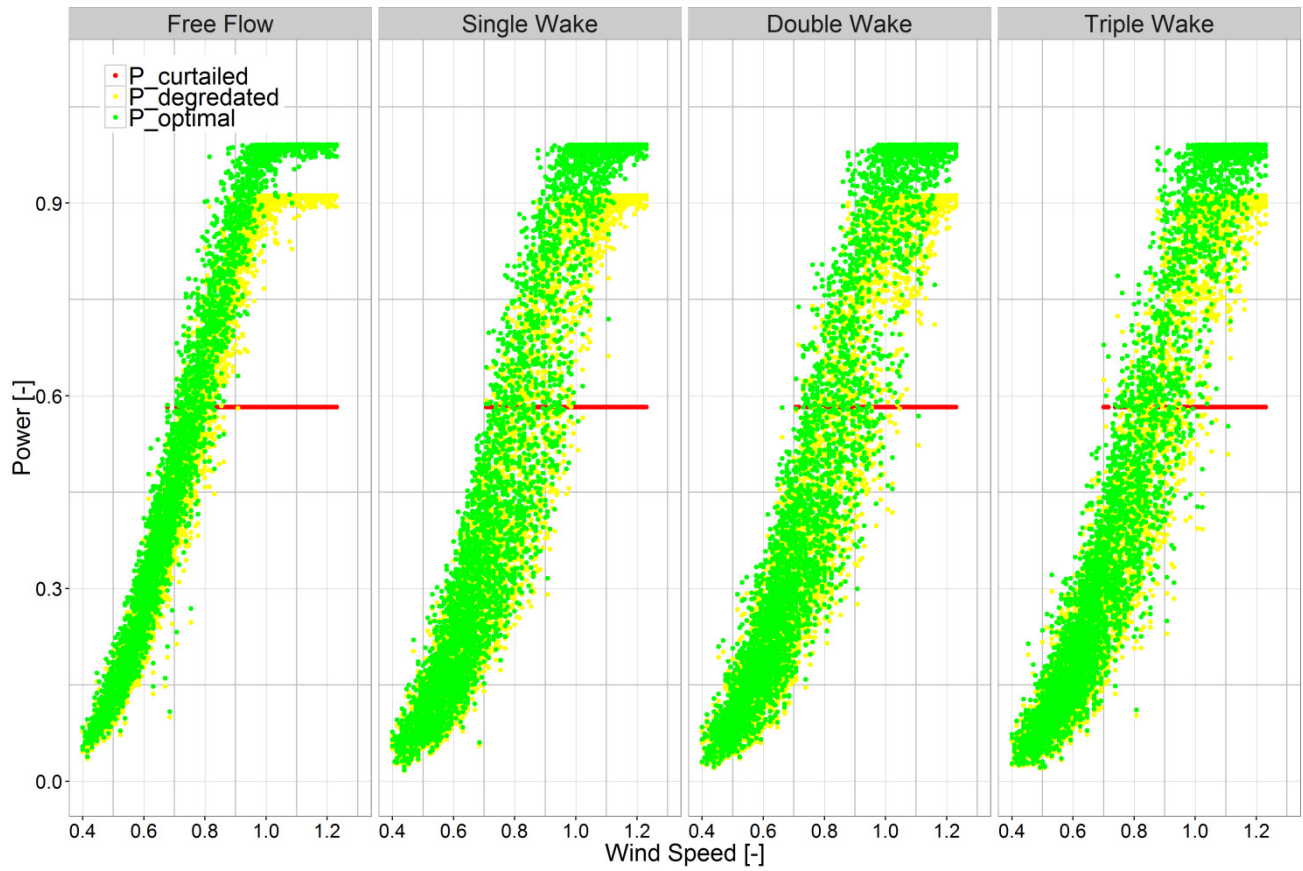
Figure 10: Scatterplot with normalized power as function of the normalized wind speed for four turbines in one row with two error test cases. Green dots are the measured power values and represent optimal operation. 8 % degradation of the power output is shown with yellow dots. A curtailment at 58 % is shown in red.
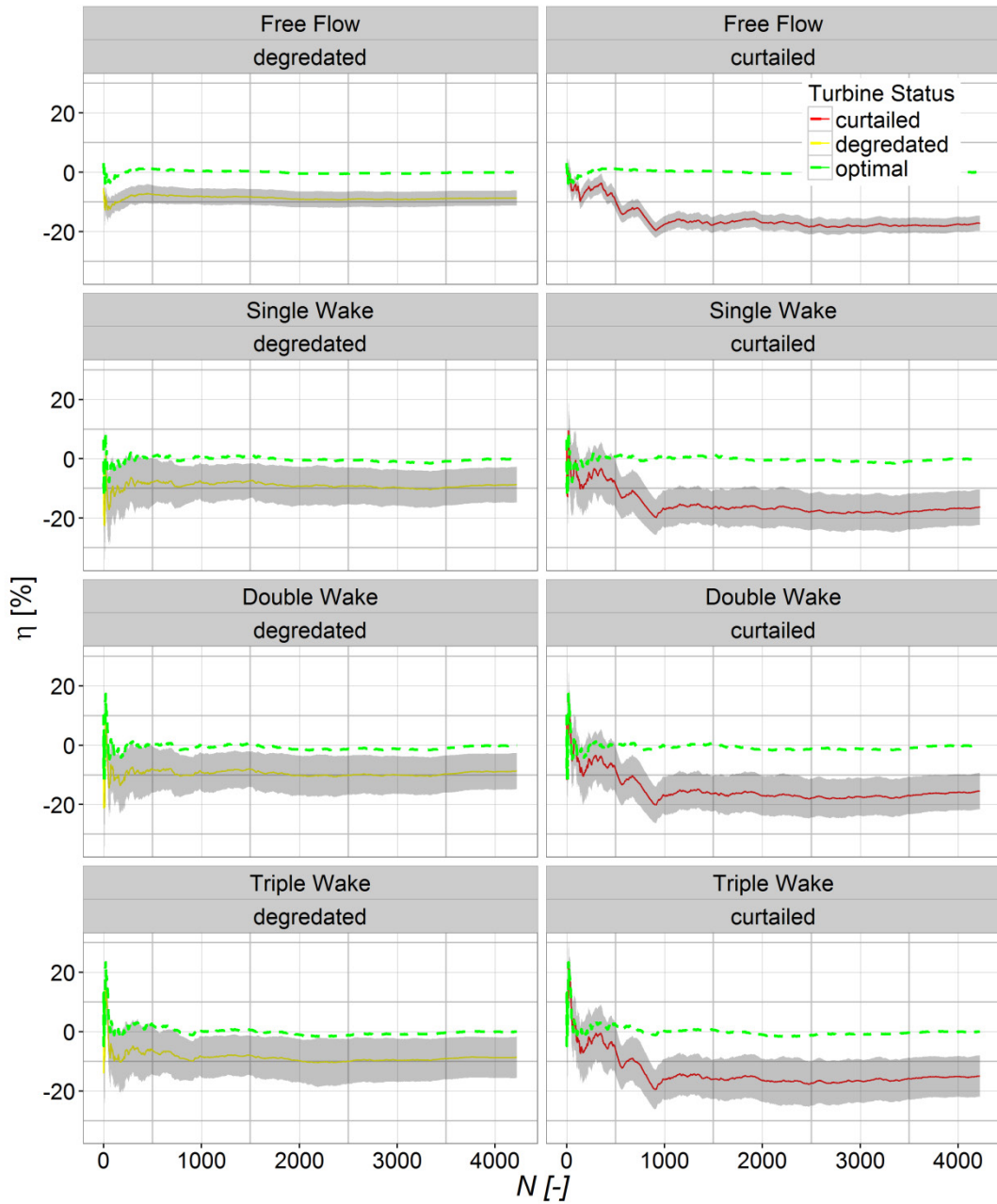
Figure 11: Underperformance detection for curtailment (right column) and degradation (left column) at turbines with different levels of wake influence. The displayed values represent the underperformance indicator η as function of the number of values N. We highlight the first time of underperformance detection when the green dotted line is outside of the grey uncertainty bandwidth.
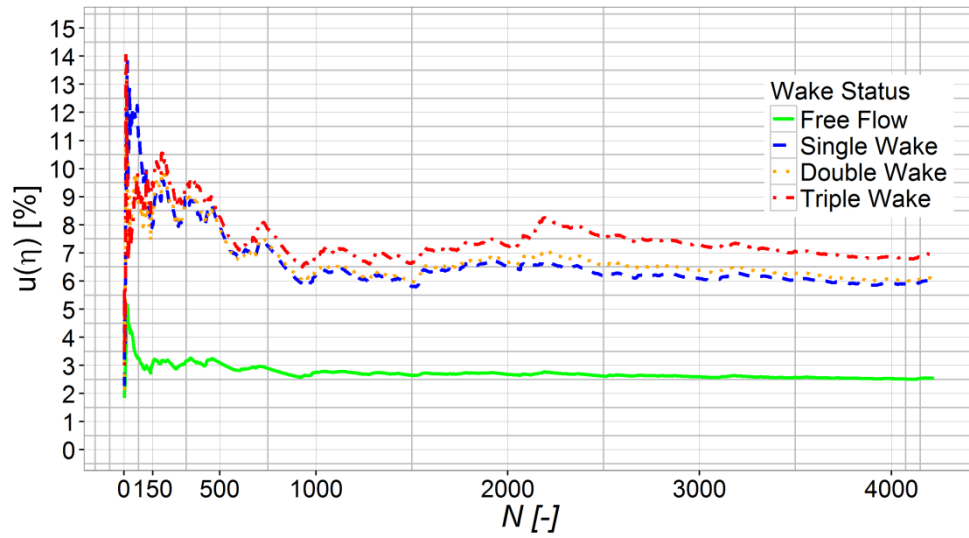
Figure 12: Uncertainties for the underperformance indicator u(η) as function of *N* values for free flow, single wake, double wake and triple wake situation. Uncertainties for free flow conditions (green) are much lower that the uncertainties for the waked turbines.
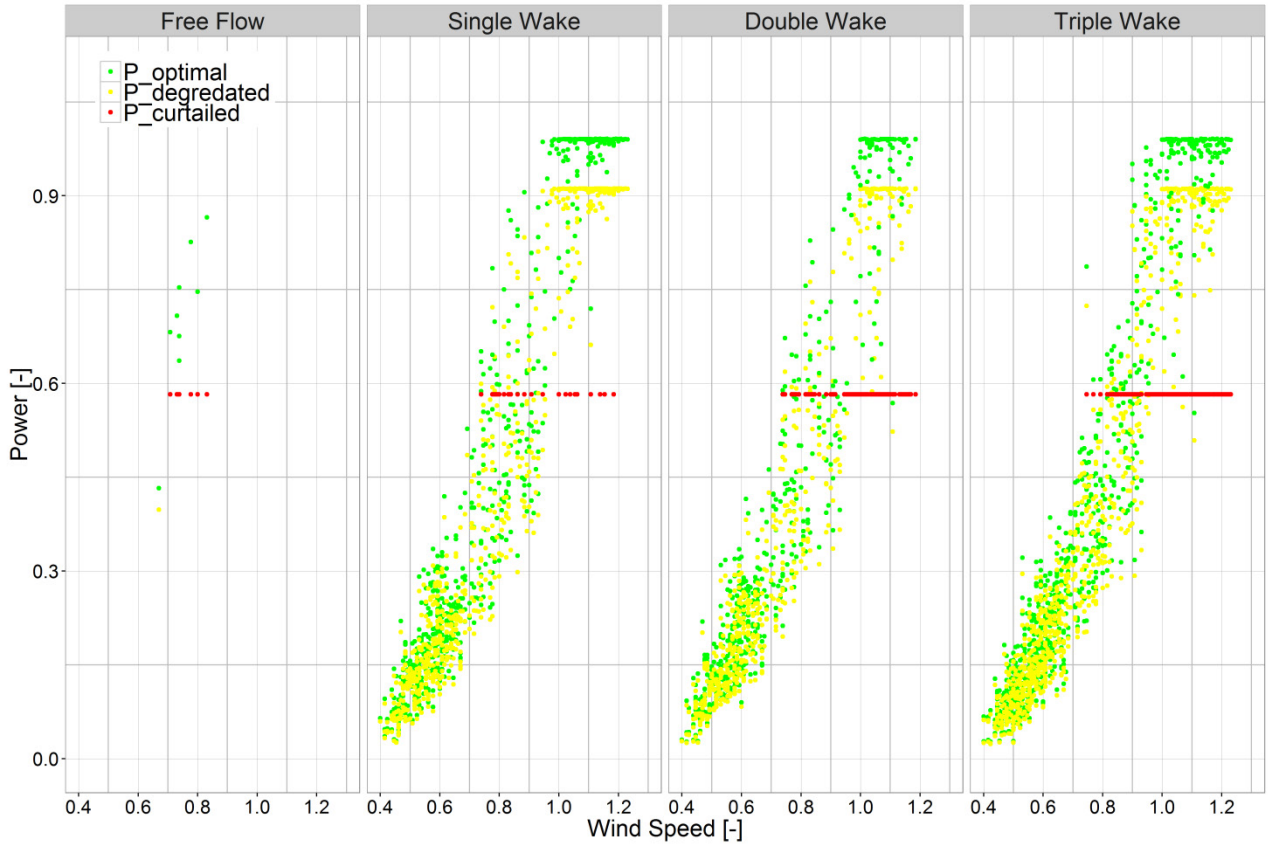
Figure 13: Scatterplot of each turbines normalized power curve. The quantity $N = 754$ equals to the estimated sample size for the first detection of degradation at a turbine in triple wake situation.

Table 1: Type B uncertainties of the predicted power P_π

k	Uncertainty Component	Sensitivity $c_{k,i,j}$	Uncertainty $u_{k,i,j}$
1	Wind speed estimation	$\left\lvert\dfrac{P_{\pi\,i,j} - P_{\pi\,i-1,j}}{V_{ij} - V_{i-1,j}}\right\rvert$	One standard deviation of the averaged anemometers
2	Wind direction estimation	$\left\lvert\dfrac{P_{\pi\,i,j} - P_{\pi\,i-1,j}}{\vartheta_{ij} - \vartheta_{i-1,j}}\right\rvert$	One standard deviation of the averaged wind direction

Table 2: Type B uncertainties of the measured power P_μ (values as suggested by IEC 61400-12-1)

k	Uncertainty Component	Sensitivity $c_{k,i,j}$	Uncertainty $u_{k,i,j}$
1	Current transformer	1	0.0043 P [kW]
2	Voltage transformer	1	0.003 P [kW]
3	Power transducer	1	0.003 P_{rated} [kW]
4	Power data acquisition	1	0.001 P_{rated} [kW]

Table 3: *N* values to the first detection of underperformance with certainty of one standard deviation. Values in brackets indicate *N* with wind speeds above the curtailment.

Wake situation	*N*_degradation [-]	*N*_curtailment [-]
Free Flow	1	51 (8)
Single Wake	577	149 (28)
Double Wake	502	501 (106)
Triple Wake	754	655 (164)

5   **Table 4:** Uncertainty *U* at quantity *N* of first detection of underperformance with certainty of one standard deviation.

Wake situation	*U*_degradation [%]	*U*_curtailment [%]
Free Flow	1.8	3.6
Single Wake	6.9	7.9
Double Wake	7.8	7.8
Triple Wake	7.8	7.3